SUPPORTING INFORMATION

Tales of Dihydrofolate Binding to R67 Dihydrofolate Reductase

Michael R. Duff, Jr.,† Shaileja Chopra, †‡
M. Brad Strader,§ Pratul K. Agarwal,†,|| and Elizabeth E. Howell†,*

†Department of Biochemistry, Cellular, & Molecular Biology, University of Tennessee, Knoxville, TN 37996-0840

‡ Present Address, University of North Carolina, Chapel Hill, NC

§Laboratory of Biochemistry and Vascular Biology, Center for Biologics Evaluation and Research, Food and Drug Administration, Bethesda, MD 20892

||Computer Science and Mathematics Division, Oak Ridge National Laboratory, Oak Ridge, TN 37831

Supplemental Figures

Histag numbering
1 11 21 31 41 51
MRGSHHHHHH GMASMTGGQQ MGRDLYDDDD KDPSSNEVSN PVAGNFVFPS NATFGMGDRV
MIRSSNEVSN PVAGNFVFPS NATFGMGDRV
Wt R67 numbering 1 11 21
61 71 81 91 101
RKKSGAAWQG QIVGWYCTNL TPEGYAVESE AHPGSVQIYP VAALERIN
RKKSGAAWQG QIVGWYCTNL TPEGYAVESE AHPGSVQIYP VAALERIN
31 41 51 61 71

Figure S1. A comparison of the protein sequence for wt R67 DHFR (black) with the Histagged variant (red). The lysines that are available for reaction with EDC are highlighted in yellow.

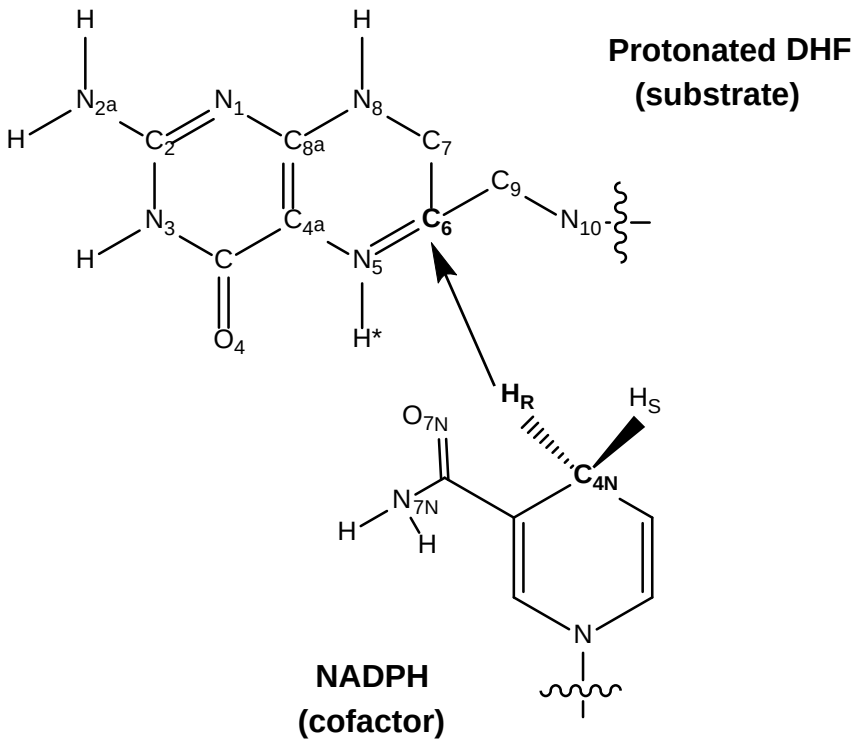

Figure S2. Structures and atom labels for the pterin ring of protonated dihydrofolate and the nicotinamide ring of NADPH.

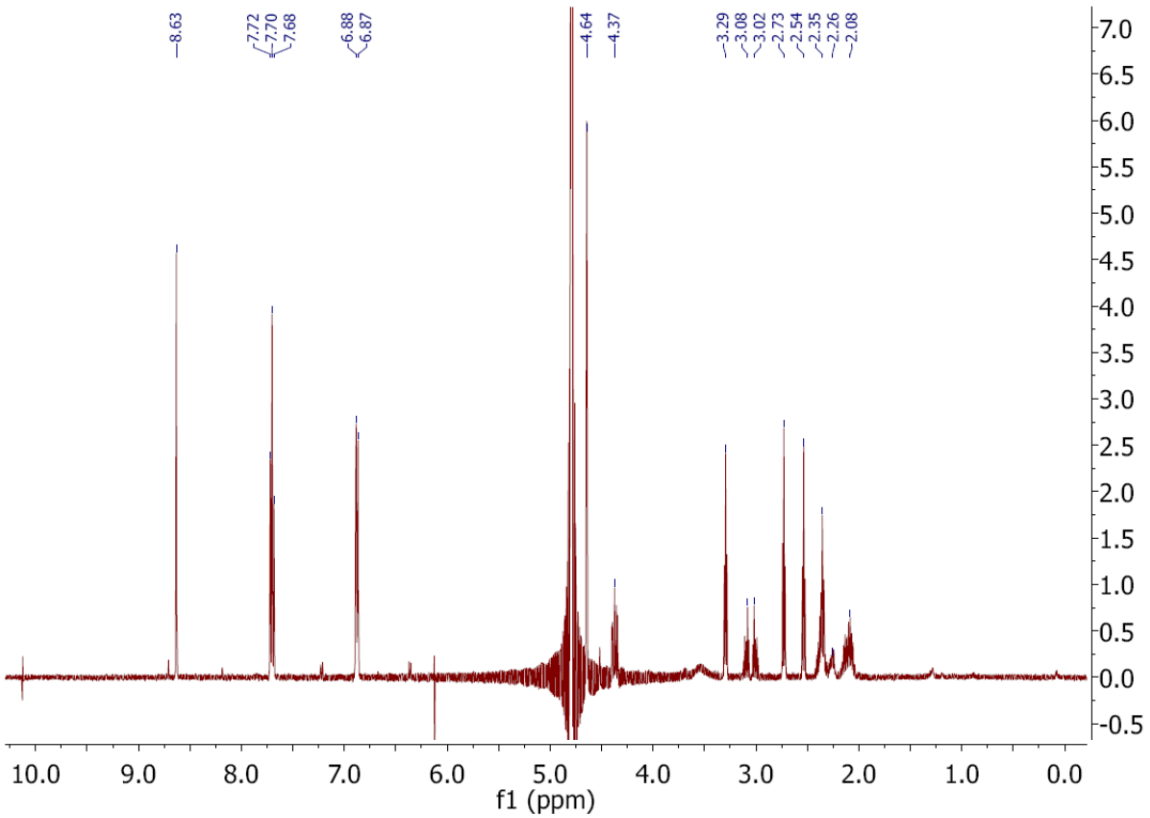

Figure S3. Proton NMR of the bis-(1-(2-aminoethyl)amide)-folate-(α,γ) adduct in D_2O. Peaks at 3.29, 3.07, 3.01, 2.73 and 2.54 arise from the conjugated ethylene diamines (EDA). Overlap of the DMSO-d peak with the EDA peaks precluded performing the NMR in DMSO-d. ^{1}H NMR (500 MHz, D2O): 8.63 (s, 1H, C7-H); 7.70 (m, 2H, C2'/C6'-H); 6.88 (m, 2H, C3'/C5'-H); 4.64 (s, 2H, C9-H); 4.4 (m, 1H, Cα-H); 3.29 (t, 2H, EDA); 3.07 (m, 1H, EDA); 3.01 (m, 1H, EDA); 2.73 (t, 2H, EDA); 2.54 (t, 2H, EDA); 2.37 (m, 2H, Cγ-H); 2.10 (m, 2H, Cβ-H). Similar NMR assignments have been previously made for conjugated folates.[1]

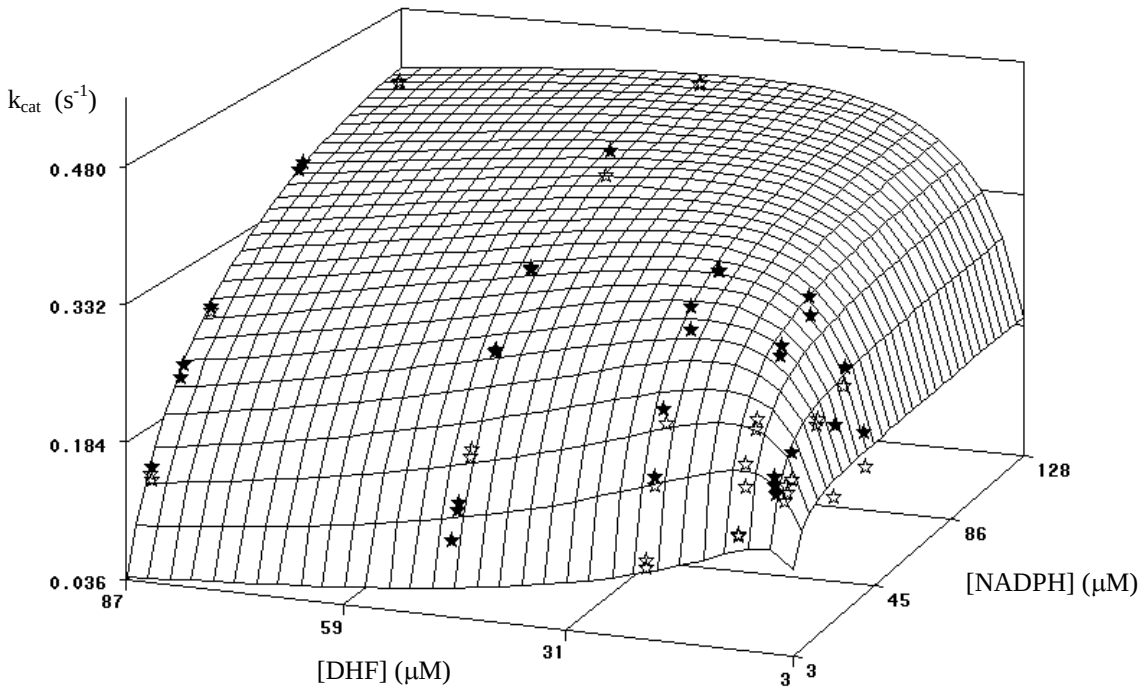

Figure S4. Steady state kinetic analysis of the I68A:3 mutation in Quad3. The SAS fits employed an equation describing a bisubstrate reaction showing substrate inhibition.[2, 3] Best fit values are given in Table 1 of the main text. The predicted values are shown by the grid lines while the data points are given by stars. Solid and hollow stars lie above and below the fit values, respectively.

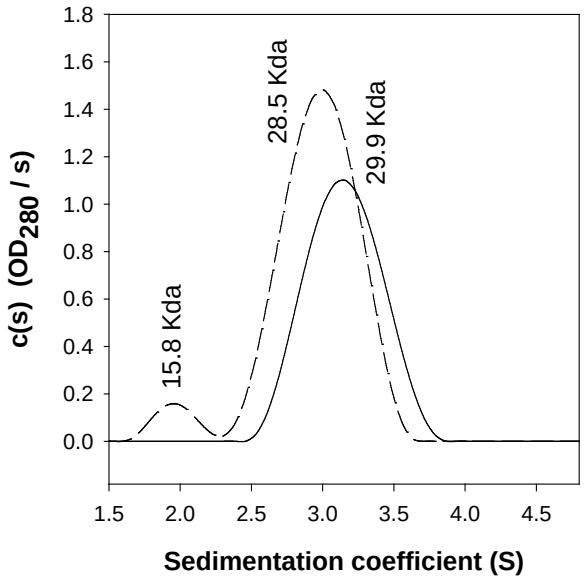

Figure S5. The concentration of discrete species, or c(s), calculated from analysis of sedimentation velocity data. Using a continuous c(s) distribution model in Sedfit[(4)], s values can be calculated and then converted to molecular masses. The data for the truncated R67 DHFR control are shown by the dashed line. The main species has an s value of 2.99, corresponding to a tetramer of mass 28,500 daltons; a small peak with an s value of 1.99 corresponds to a dimer of mass 15,800 daltons. The data describing the crosslinked sample (folate plus truncated R67 DHFR) are shown by a solid line. The peak describes a species with an s value of 3.15 and a mass of 29,920 Da.

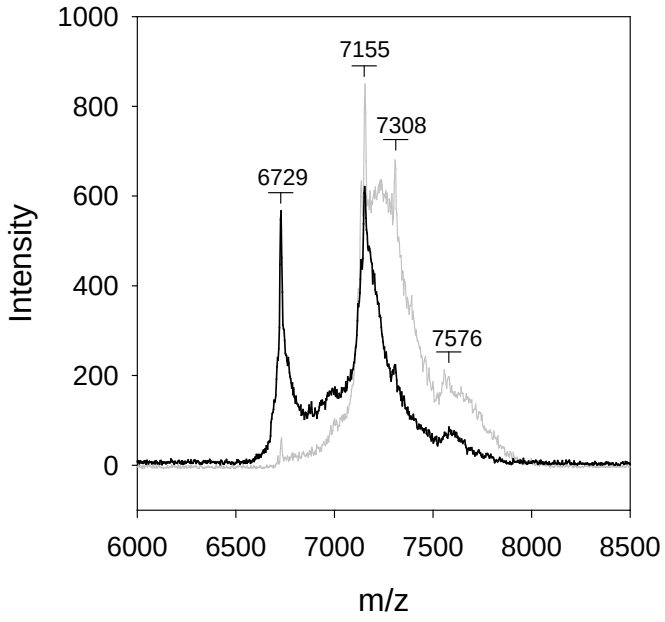

Figure S6. Mass spectra of truncated R67 DHFR crosslinked with folate and EDC. The black spectrum describes a reaction using a low folate concentration (72μM) which had ~25% activity remaining. While dimer peaks were also noted, this analysis focuses on the monomer. The prominent peak at a m/z of 6729 corresponds to the unmodified truncated protein while the folate adduct appears at 7155. The gray spectrum corresponds to a reaction run at a higher folate concentration (150μM) which had <10% activity remaining. The peak for unmodified, truncated protein is greatly diminished while the folate adduct peaks are much more prominent. The peak at 7308 likely corresponds to a species containing both folate and EDC adducts. The peak near 7576 is consistent with a species with 2 crosslinked folates per monomer.

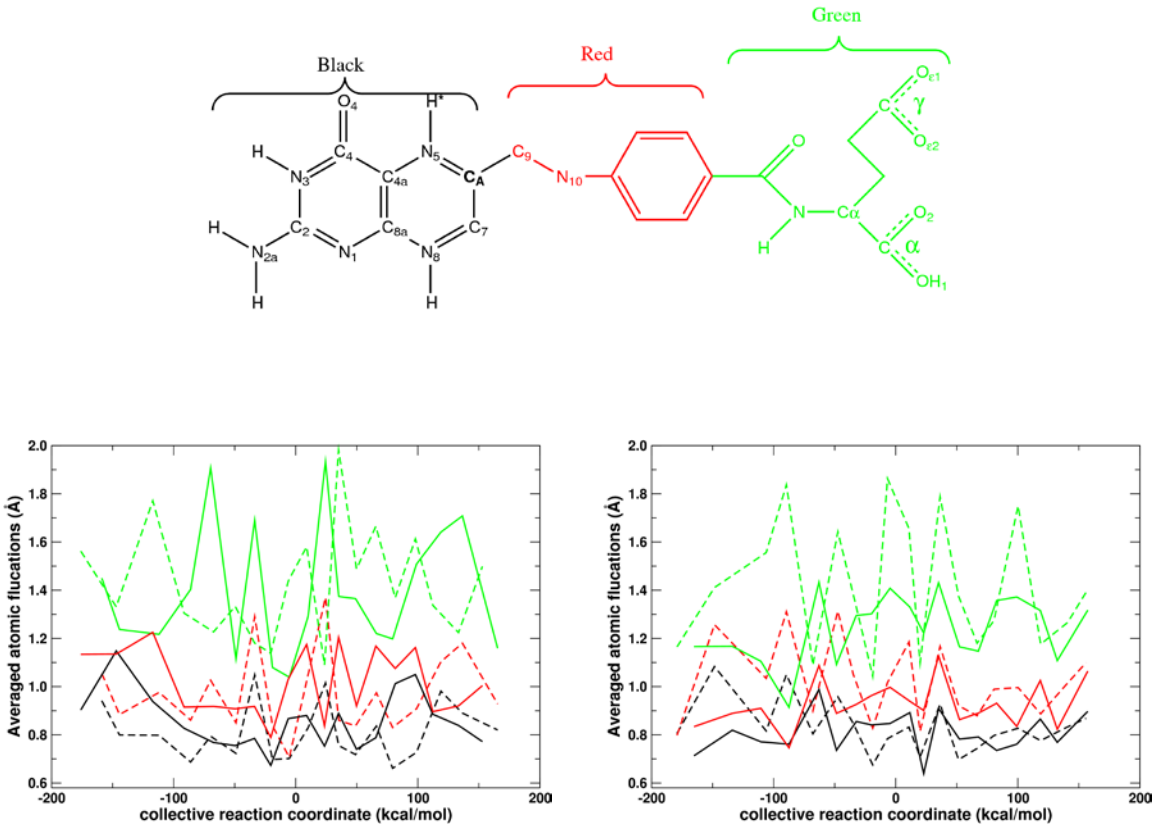

Figure S7. Molecular dynamics analysis of the hydride transfer reaction catalyzed by R67 DHFR. A weak restraint between the carbon atom of the DHF γ-carboxylate and the N_ε atom of the K32:3 side-chain was applied to tether the substrate near the lysine (see main manuscript for details). Two independent simulations were performed and named EVB1 (left panel) and EVB2 (right panel). Solid lines indicate MD simulations with restraints. For comparison, fluctuations from simulation with the free tail (without any restraints) are shown as dashed lines. The top image colors the sections of protonated dihydrofolate that were monitored (pterin ring, black; C9-N10-phenyl, red and O=C-glutamate, green) and the bottom images show the averaged atomic fluctuations along the collective reaction coordinate, color coded according to the moiety monitored.

pK_a calculations While K32 occurs on the edge of the active site pore and is exposed to solvent, it is also near a positively charged patch of amino acids, including R29, R31, K33, and R76. While counter charges also occur nearby (D28, E58, E60 and E75), a positively charged electrostatic potential has been proposed to facilitate binding of the negatively charged ligands.[5] To gain some insight into whether the pK_a for K32 might be altered by its environment, Macrodox was used to calculate pK_a values based on a Tanford-Kirkwood continuum electrostatic model.[6-8] The calculated pK_a for K32 in the apo enzyme is 10.4, indicating no large effect on the pK_a value. Macrodox calculates the pK_a for K33 as 10.5 and the pK_a for the N-terminus at Pro19 in the 1VIE crystal structure as 8.19.

SDS-PAGE experiments As mentioned in the manuscript, SDS-PAGE of folate crosslinked protein showed the predominant species was monomeric, however higher order oligomers were also seen. One possibility is that a specific crosslink occurs between one of the carboxylates in folate and K32, followed by reaction of the remaining folate carboxylate with one of the N-termini in the tetramer. This option seems likely as the N-terminus might be expected to be more reactive than any remaining lysine sidechains due to its lower pK_a. Also, as the 17 N-terminal amino acids are disordered in the dimer crystal structure, [9] the flexibility of the N-terminus could transiently position it near the remaining folate carboxylate group.

To determine if the N-terminus is involved in the intermolecular crosslinking event(s), R67 DHFR was truncated using chymotrypsin.[10, 11] Truncated R67 DHFR is fully active and the new N-terminus at V17 is not close enough to bound folate to form a crosslink. Analysis of the crosslinked species via SDS-PAGE showed both monomers and dimers. While the intensity of the dimer band was clearly decreased, it was not eliminated, suggesting the N-terminus is only partly responsible for the intermolecular reaction.

Another possibility explaining formation of intermolecular crosslinks is that EDC allows bond formation between carboxylates in one R67 DHFR monomer (E7, D28, E53, E58, E60, E75) and amines in another monomer. This hypothesis was investigated by incubating truncated R67 DHFR with only EDC. Dimer bands in SDS-PAGE were noted after overnight incubation, consistent with EDC being able to cause non-folate dependent intermolecular crosslinks.

Reduction of the tethered folate was observed. Was this event intramolecular or intermolecular? While it is possible that the crosslinked folate from one R67 DHFR molecule could be reduced by a second R67 DHFR tetramer, this seems unlikely as not all the crosslinked folate was reduced. Also folate crosslinking stabilizes the tetramer (see Figure 3), suggesting additional contacts between the ligand and the protein. This scenario supports a species where folate is docked in the active site rather than being accessible in solution to another R67 molecule. Additionally, a K_m effect for folate-R67 to bind to a second R67 molecule would be expected if an intermolecular reduction reaction occurred. For this case, it seems likely that the bulky protein appendage would greatly weaken binding of crosslinked folate to a second R67 by a steric effect.

Asymmetric K32M mutants We have previously constructed asymmetric K32M mutations in a tandem array of four fused R67 DHFR genes.[12, 13] Double mutants have 3 possible configurations, K32M:1+2, K32M:1+3 and K32M:1+4. The below cartoon shows the K32M:1+2 and K32M:1+4 double mutants have K32M mutations on both sides of the active site pore but with different relative positions. The K32M:1+3 double mutant places both substitutions in the same half pore. As NADPH prefers to bind first and to form two salt bridges, it likely binds to the wt half pore in the K32M:1+3 mutant. This forces DHF to enter the mutant half pore. DHF K_m values for these mutants are listed in supplemental Table S1 below.

K32M:1+2

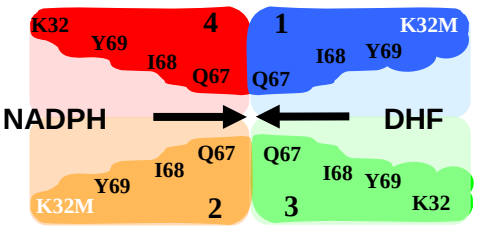

K32M:1+3

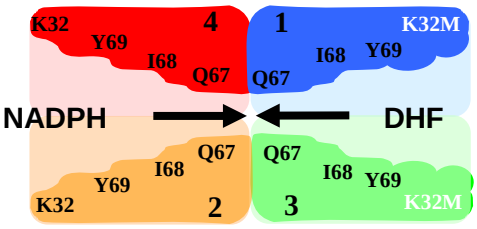

K32M:1+4

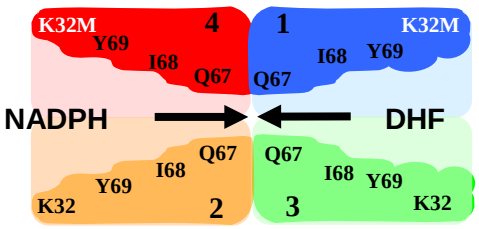

Figure S8. The R67 DHFR structure presented as a cartoon. A slice through the central pore of R67 DHFR is shown with the same orientation as in Figure 1B in the main manuscript and the color code as in Figure 1A. The residues lining the active site pore are labeled in black as is each monomer (1-4). The pore is depicted by the lighter color. The predicted positions of the asymmetric mutations are indicated in white font. For example, the K32M:1+2 mutations at the top of the figure lie on opposite sides of the pore and in a diagonal position to each other. The K32M:1+4 mutations also lie on opposite sides of the pore, but on the same side of the inter-domain β-barrel structure. The K32M:1+3 double mutant has both mutations on one side of the pore. The other side of the pore has 2 wildtype K32 residues.

Supplemental Table S1 for K_i and K_m values plotted in Figure 6 of the manuscript

Compound	Ligand net charge	K_i (μM)
PG4 [a]	-5	28 ± 2.1
PG2 [a]	-3	26 ± 1.9
Folate	-2	16 ± 3
Pteroyl-histidine [a]	-1	37 ± 3.9
Pteroyl-ornithine [a]	0	28 ± 2.2
Bis-EDA-folate	+2	140 ± 15
	# of K32 residues in half pore available for DHF binding	DHF K_m
Quad3 and Quad4 [b]	2	7.6 ± 0.4 5.6 ± 0.3
K32M:1+2 in Quad3[b]	1	14.4 ± 0.1
K32M:1+4 in Quad3[b]	1	10.5 ± 0.3
K32M:1+3 in Quad4 [b]	0	165 ± 14

[a] Ki values from Jackson et al., reference *(14)*
[b] K_m values from Feng et al. and Hicks et al. references *(12, 13)*

References for Supporting Information

1. Wang, S., Luo, J., Lantrip, D. A., Waters, D. J., Mathias, C. J., Green, M. A., Fuchs, P. L., and Low, P. S. (1997) Design and synthesis of [111In]DTPA-folate for use as a tumor-targeted radiopharmaceutical, *Bioconjugate chemistry 8*, 673-679.
2. Smiley, R. D., Stinnett, L. G., Saxton, A. M., and Howell, E. E. (2002) Breaking symmetry: mutations engineered into R67 dihydrofolate reductase, a D2 symmetric homotetramer possessing a single active site pore, *Biochemistry 41*, 15664-15675.
3. Smiley, R. D., Saxton, A. M., Jackson, M. J., Hicks, S. N., Stinnett, L. G., and Howell, E. E. (2004) Nonlinear fitting of bisubstrate enzyme kinetic models using SAS computer software: application to R67 dihydrofolate reductase, *Anal. Biochem. 334*, 204-206.
4. Schuck, P. (2000) Size-distribution analysis of macromolecules by sedimentation velocity ultracentrifugation and lamm equation modeling, *Biophys. J. 78*, 1606-1619.
5. Howell, E. E., Shukla, U., Hicks, S. N., Smiley, R. D., Kuhn, L. A., and Zavodszky, M. I. (2001) One site fits both: a model for the ternary complex of folate + NADPH in R67 dihydrofolate reductase, a D_2 symmetric enzyme, *J. Comput. Aided Mol. Des. 15*, 1035-1052.

6. Tanford, C., and Kirkwood, J. G. (1957) Theory of Protein Titration Curves. I. General Equations for Impenetrable Spheres *J. Am. Chem. Soc. 79*, 5333–5339.
7. Macrodox, see http://iweb.tntech.edu/macrodox/macrodox.html ed., MacroDox was co-authored by: Dr. Scott H. Northrup, George P. Stevenson, Theo L. Laughner, Andy Boswell and Kiran Mukhyala , see http://iweb.tntech.edu/macrodox/macrodox.html.
8. Northrup, S. H., Boles, J. O., and Reynolds, J. C. L. (1987) Electrostatic effects in the Brownian dynamics of association and orientation of heme proteins, *J. Phys. Chem. 91*, 991-5998.
9. Matthews, D. A., Smith, S. L., Baccanari, D. P., Burchall, J. J., Oatley, S. J., and Kraut, J. (1986) Crystal structure of a novel trimethoprim-resistant dihydrofolate reductase specified in *Escherichia coli* by R-plasmid R67, *Biochemistry 25*, 4194-4204.
10. Reece, L. J., Nichols, R., Ogden, R. C., and Howell, E. E. (1991) Construction of a synthetic gene for an R-plasmid-encoded dihydrofolate reductase and studies on the role of the N-terminus in the protein, *Biochemistry 30*, 10895-10904.
11. Narayana, N., Matthews, D. A., Howell, E. E., and Nguyen-huu, X. (1995) A plasmid-encoded dihydrofolate reductase from trimethoprim-resistant bacteria has a novel D2-symmetric active site, *Nat. Struct. Biol. 2*, 1018-1025.
12. Hicks, S. N., Smiley, R. D., Stinnett, L. G., Minor, K. H., and Howell, E. E. (2004) Role of Lys-32 residues in R67 dihydrofolate reductase probed by asymmetric mutations, *J. Biol. Chem. 279*, 46995-47002.
13. Feng, J., Grubbs, J., Dave, A., Goswami, S., Horner, C. G., and Howell, E. E. (2010) Radical redesign of a tandem array of four R67 dihydrofolate reductase genes yields a functional, folded protein possessing 45 substitutions, *Biochemistry 49*, 7384-7392.
14. Jackson, M., Chopra, S., Smiley, R. D., Maynord, P. O., Rosowsky, A., London, R. E., Levy, L., Kalman, T. I., and Howell, E. E. (2005) Calorimetric studies of ligand binding in R67 dihydrofolate reductase, *Biochemistry 44*, 12420-12433.